Silver(I) complexation of linked 2,2'-dipyridylamine derivatives. Synthetic, solvent extraction, membrane transport and X-ray structural studies

Bianca Antonioli,[a,b] David J. Bray,[b] Jack K. Clegg,[b] Kerstin Gloe,[a] Karsten Gloe,[a*] Olga Kataeva,[a,c] Leonard F. Lindoy,[b*] John C. McMurtrie,[b] Peter J. Steel,[d*] Christopher J. Sumby,[d] Marco Wenzel[a]

[a] *Department of Chemistry, Technical University Dresden, 01062 Dresden, Germany*

[b] *Centre for Heavy Metals Research, School of Chemistry, University of Sydney, NSW, 2006, Australia*

[c] *A. E. Arbuzov Institute of Organic and Physical Chemistry, Kazan 420088, Russia*

[d] *Department of Chemistry, University of Canterbury, Christchurch, New Zealand*

Abstract

Synthesis of the 2,2'-dipyridylamine derivatives di-2-pyridylaminomethylbenzene **1**, 1,2-bis(di-2-pyridylaminomethyl)benzene **2**, 1,3-bis(di-2-pyridylaminomethyl)benzene **3**, 2, 6-bis(di-2-pyridylaminomethyl)pyridine **4**, 1,4-bis(di-2-pyridylaminomethyl)benzene **5**, and 1,3,5-tris(di-2-pyridylaminomethyl)benzene **6** are reported together with the single crystal X-ray structures of **2**, **3**, and **5**. Reaction of individual salts of the type AgX (where X = NO_3^-, PF_6^-, ClO_4^-, or BF_4^-) with the above ligands has led to the isolation of thirteen Ag(I) complexes, nine of which have also been characterised by X-ray

diffraction. In part, the inherent flexibility of the respective ligands has resulted in the adoption of a range of coordination arrangements. A series of liquid-liquid ($H_2O/CHCl_3$) extraction experiments of Ag(I) with varying concentrations of **1-6** in the organic phase have been undertaken, with the counter ion in the aqueous phase being respectively picrate, perchlorate and nitrate. In general, extraction efficiencies for a given ionophore followed the Hofmeister order of picrate>perchlorate>nitrate; in each case the tris-dpa derivative **6** acting as the most efficient extractant of the six systems investigated**.** Competitive seven-metal bulk membrane transport experiments ($H_2O/CHCl_3/H_2O$) employing the above ligands as the ionophore in the organic phase and equimolar concentrations of Co(II), Ni(II), Zn(II), Cu(II), Cd(II), Pb(II) and Ag(I) in the aqueous source phase were also undertaken, with transport occurring against a pH gradient. Under the conditions employed **1** and **5** yielded negligible transport of any of the metals present in the source phase while sole transport selectivity for Ag(I) was observed for **2-4** and **6**.

Introduction

The coordination chemistry of 2,2´-dipyridylamine (dpa) and its derivatives has been the focus of a considerable number of investigations. For example, mono-, di- and tri-dpa derivatives have been reported in which the secondary nitrogen of each dpa is directly bound to an aryl core with such species being employed in studies that range from metal coordination and supramolecular chemistry[1,2] to the synthesis of new luminescent materials.[3-5] Pd(II) and Pt(II) complexes of such dpa derivatives have also been

investigated as potential anticancer agents due to their structural similarity to cis-platin.[6-8] The use of Ag(I) in a range of metal complex and supramolecular materials has received increasing attention, in part due to the coordination flexibility of this d^{10} ion and its well documented tendency to form strong complexes with nitrogen donor ligands.[9] Further, the silver centres in such materials have frequently been associated with 'supramolecular' interactions (including silver-π interactions)[10,11] and in some instances give rise to unusual electronic and photophysical properties.[12]

In the above context, the dpa moiety has been demonstrated to coordinate to Ag(I) and the solid state structure of [Ag(deprotonated dpa)]$_n$ has been reported.[13] Under the synthetic conditions employed, deprotonation of the central amine nitrogen occurs resulting in a charge-neutral, one dimensional polymeric chain, with the backbone of the chain defined by weak Ag-Ag interactions; each silver ion is coordinated to an amido nitrogen as well as two pyridyl nitrogens from three different dpa ligands. Under other reaction conditions, neutral dpa has also been shown to form discrete complexes with silver.[14] In each of these latter systems the secondary amine nitrogen does not coordinate to silver and each dpa unit acts as a bidentate ligand, coordinating through both pyridyl nitrogens to form a six-membered chelate ring. Coordination to silver solely through pyridyl nitrogen donors is also typical of other substituted dpa ligands.[2,4,15]

In contrast to the above systems, examples of linked di- and tri-dpa derivatives in which the linking groups between the dpa fragments are flexible have not been extensively studied.[7,8,16] Nevertheless, complexes of such flexible poly-dpa derivatives bound to Cu(II),[16] as well as Pd(II) and Pt(II),[7,8] have been investigated for use in biological applications. However, no silver complexes of dpa derivatives of this type

have been described previously and this, in part, provided one motivation for the present study.

We now report a comparative solid state and solution investigation of the interaction of the linked 2,2´-dipyridylamine ligand systems **1**–**6** with Ag(I).

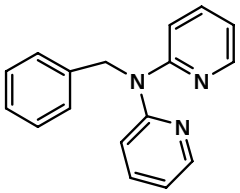

1

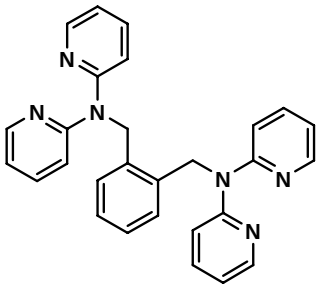

2

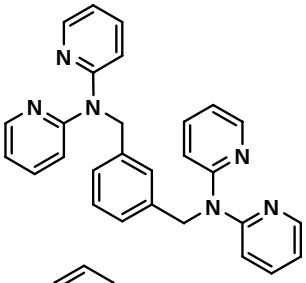

3

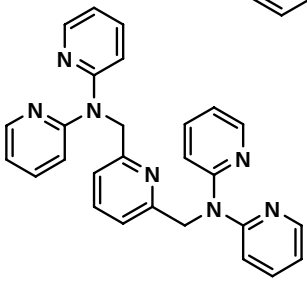

4

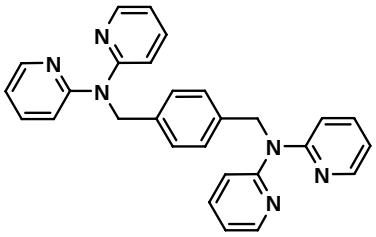

5

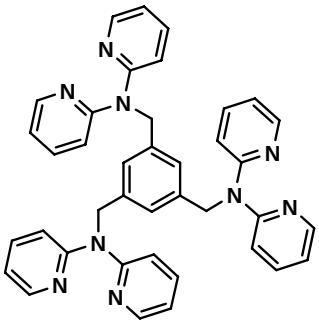

6

Experimental

Physical methods

HRMS were determined on samples loaded in dichloromethane and run in an acetonitrile matrix. Column chromatography was performed on silica gel 60 (0.040–0.063 mm Merck) or neutral Al_2O_3 (FH 300 mm, HNS 29 Por.0). Melting points are uncorrected. NMR spectra were determined on a DRX-500 Bruker spectrometer or on Varian 300 and 500 MHz spectrometers.

Ligand synthesis

Di-2-pyridylaminomethylbenzene (1)

This synthesis was based on literature procedures.[17] Benzylbromide (1.0 g, 5.88 mmol) in DMF (3 mL) was added dropwise to 2,2'-dipyridylamine (1.0 g, 5.85 mmol) and KOH (1.33 g, 23.7 mmol) in DMF (5 mL). The resulting solution was stirred at room temperature for 15 h and then taken to dryness under reduced pressure. The residue was washed with excess water and extracted with chloroform (3 × 50 mL). The chloroform extracts were dried over anhydrous sodium sulfate, filtered, and the filtrate taken to dryness under reduced pressure. The residue was chromatographed on silica gel by elution with $CHCl_3$/MeOH (5 : 1). The crude yellow product obtained was recrystallised from an acetone/water mixture. Yield, 0.25 g (16 %); mp 76.5 °C. Found: C, 78.01; H: 5.72; N: 16.12. Calc. for $C_{17}H_{15}N_3$: C, 78.13; H, 5.79; N, 16.08 %.

^{1}H NMR (500 MHz; $CDCl_3$; 298K) δ 8.40 (2H, d, py), 7.60 (2H, t, py), 7.37 (2H, d, py), 7.27 (2H, d, ph), 7.20 (1H, t, ph), 7.16 (2H, d, ph), 6.94 (2H, t, py), 5.55 (2H, s, CH_2)
MS (ESI) m/z = 262.1 $[M+H]^+$.

1,2-Bis(di-2-pyridylaminomethyl)benzene (2)

Di-2-pyridylamine (1.00 g, 5.84 mmol) and potassium hydroxide (1.33 g, 23.7 mmol) were stirred in DMSO (5 mL) for 1 h; 1,2-bis(bromomethyl)benzene (0.70 g, 2.65 mmol) was added and the reaction mixture was stirred for a further 40 h. Water was then added until the solution turned cloudy. The yellow precipitate that formed was isolated and recrystallised from an ethyl acetate-petroleum ether solution to yield yellow crystals. Yield, 0.29 g (25 %); mp 144-146 ºC. Found: C, 75.37; H, 5.38; N, 19.04. Calc. for $C_{28}H_{24}N_6$: C, 75.65; H, 5.44; N, 18.91 %. ^{1}H NMR (500 MHz, $CDCl_3$, 296 K) δ: 8.32 (4H, d, py), 7.53 (4H, t, py), 7.27 (2H, d, ph), 7.22 (4H, d, py), 7.04 (2H, t, ph), 6.86 (4H, dd, py), 5.64 (4H, s, CH_2). ^{13}C NMR (125.76 MHz, $CDCl_3$, 296 K) δ: 157.1, 148.2, 137.2, 136.1, 126.5, 117.2, 114.6, 48.6. MS (HR-ESI): 444.2079; $C_{28}H_{24}N_6$ requires 444.2063.

1,3-Bis(di-2-pyridylaminomethyl)benzene (3)

Di-2-pyridylamine (1.00 g, 5.84 mmol) and potassium hydroxide (1.33 g, 23.7 mmol) were stirred in DMF (30 mL) at 40 ºC for 20 min. 1,3-Bis(bromomethyl)benzene (0.699 g, 2.65 mmol) was added and stirring was continued at 40 ºC for a further 40 h. The solvent was removed under reduced pressure and the residue partitioned between dichloromethane (200 mL) and water (150 mL). The organic layer was washed twice with water (2 x 150 mL) and then the combined aqueous phases washed with dichloromethane (2 x 100 mL). The combined dichloromethane layers were dried (Na_2SO_4) and then evaporated, resulting in a pale yellow solid. This was recrystallised from acetone/water yielding 980 mg (83 %) of a yellow crystalline solid; mp 133-134 ºC.

Found: C, 75.46; H, 5.49; N, 19.03. Calc. for $C_{28}H_{24}N_6$: C, 75.65; H, 5.44; N, 18.91 %. ^{1}H NMR (500 MHz, $CDCl_3$, 296 K) δ: 8.25 (4H, d, py), 7.53 (4H, t, py), 7.27 (2H, d, ph), 7.22 (4H, d, py), 7.04 (2H, t, py), 6.86 (4H, t, py), 5.64 (4H, s, CH_2). ^{13}C NMR (500MHz, $CDCl_3$, 296 K) δ: 157.1, 148.2, 137.2, 136.1, 126.5, 117.2, 114.6, 48.62. MS (HR-ESI): 444.20638; $C_{28}H_{24}N_6$ requires 444.20638.

2,6-Bis(di-2-pyridylaminomethyl)pyridine (4)

This was synthesised and characterised as described elsewhere.[18]

1,4-Bis(di-2-pyridylaminomethyl)benzene (5)

Di-2-pyridylamine (1.00 g, 5.84 mmol) and potassium hydroxide (1.33 g, 23.7 mmol) were stirred in DMF (30 mL) at 40 °C for 20 min. 1,3-Bis(bromomethyl)benzene (0.699 g, 2.65 mmol) was added and stirring was continued at 40 °C for a further 40 h. The solvent was removed under reduced pressure and the residue partitioned between dichloromethane (200 mL) and water (150 mL). The organic layer was washed twice with water (2 x 150 mL) and then the combined aqueous phases washed with dichloromethane (2 x 100 mL). The combined dichloromethane layers were dried (Na_2SO_4) and then evaporated, resulting in a pale yellow solid. This was recrystallised from acetone/water yielding 780 mg (66 %) as a yellow powder; mp 181-183 °C. Found: C, 75.47; H, 5.44; N, 19.01. Calc. for $C_{28}H_{24}N_6$: C, 75.65; H, 5.44; N, 18.91 %. ^{1}H NMR (500 MHz, $CDCl_3$, 296 K) δ: 8.28 (4H, d, py), 7.47 (4H, t, py), 7.22 (4H, s, ph), 7.13 (4H, d, py), 6.82 (4H, dd, py), 5.43 (4H, s, CH_2). ^{13}C NMR (500 MHz, $CDCl_3$, 296 K) δ:

157.1, 148.1, 137.6, 137.1, 126.9, 117.1, 114.5, 51.02. MS (HR-ESI): 444.2078; $C_{28}H_{24}N_6$ requires 444.2063.

1,3,5-Tris(di-2-pyridylaminomethyl)benzene (6)

This was prepared by an adaptation of a published procedure.[7] Di-2-pyridylamine (1.00 g, 5.84 mmol) and potassium hydroxide (1.31 g, 23.4 mmol) were stirred in DMSO (5 mL) for 1 h. 1,3,5-Tris(bromomethyl)benzene[19] (0.675 g, 1.89 mmol) was then added and the solution stirred for an additional 48 h. Water was added dropwise until the solution turned cloudy. On standing, a yellow precipitate formed which was filtered off, washed with water and recrystallised from an ethyl acetate-petroleum ether mixture. Yield, 0.583 g (49 %); mp 158-160 ºC. Found: C, 74.33; H, 5.07; N, 19.80. Calc. for $C_{39}H_{33}N_9$: C, 74.62; H, 5.30; N, 20.08 %. ^{1}H NMR (500 MHz, $CDCl_3$, 296 K) δ: 8.20 (6H, d, py), 7.37 (6H, t, py), 7.07 (3H, s, ph), 6.91 (6H, d, py), 6.78 (6H, dd, py), 5.34 (6H, s, CH_2). ^{13}C NMR (125.76 MHz, $CDCl_3$, 296 K) δ: 157.0, 148.0, 139.4, 137.0, 123.6, 116.9, 114.5, 51.18. MS (HR-ESI): 628.2937. $C_{39}H_{34}N_9^+$ requires 628.2953.

Complex synthesis

CAUTION. Perchlorate complexes are potentially explosive and appropriate caution should be exercised in their synthesis and handling.

*[Ag(**1**)(NO_3)]·CH_3CN*

Silver nitrate (13.3 mg, 0.078 mmol) in acetonitrile (5 mL) was added to **1** (20.5 mg, 0.078 mmol) in dichloromethane (5 mL). Colourless crystals of the title compound were

obtained by slow diffusion of diethylether vapour into the resulting solution. The crystals were collected and washed with ether. Yield, 10.0 mg (76 %); mp 160-162 °C (dec.). Found: C, 48.17; H, 3.65; N, 14.79. Calc. for $C_{17}H_{15}N_4AgO_3 \cdot CH_3CN$: C, 48.32; H, 3.84; N, 14.68 %.

$[Ag_2(\mathbf{2})_2(NO_3)_2] \cdot 2H_2O$

Silver nitrate (0.168 g, 0.099 mmol) in methanol (5 mL) was added to **2** (0.201 g, 0.045 mmol) in dichloromethane/methanol (1:1; 8 mL). Colourless crystals that were suitable for X-ray crystallography formed on slow evaporation of the resulting solution. These were collected, washed with dichloromethane and methanol, and dried under vacuum. Yield, 25.2 mg (89%); mp 233-235 ºC (dec.). Found: C, 53.32; H, 3.71; N, 15.87. Calc. for $C_{56}H_{48}Ag_2N_{14}O_6 \cdot 2H_2O$: C, 53.18; H, 4.14; N, 15.50 %.

$[Ag_2(\mathbf{2})_2(ClO_4)_2] \cdot CH_3CN$

Silver perchlorate (13.0 mg, 0.063 mmol) in acetonitrile (5 mL) was added to **2** (14.1 mg, 0.031 mmol) in dichloromethane (5 mL). Colourless crystals of the title compound were obtained by slow diffusion of diethylether vapour into the resulting solution. The crystals were collected, washed with ether, and dried under vacuum. Yield, 10.3 mg (79 %); mp 230-232 °C. Found: C, 51.75; H, 3.68; N, 13.79. Calc. for $C_{56}H_{48}Ag_2Cl_2N_{12}O_8 \cdot CH_3CN$: C, 51.51; H, 3.82; N, 13.54 %.

$[Ag_2(\mathbf{2})_2](BF_4)_2$

Silver tetrafluoroborate (18.7 mg, 0.096 mmol) in methanol was added to **2** (20.2 mg, 0.045 mmol) in dichloromethane/methanol (1:1; 8 mL). The colourless crystals that formed were collected, washed with dichloromethane and methanol. These crystals were suitable for X-ray crystallography. The remaining crystals were dried under vacuum before microanalysis. Yield 17.4 mg (60%); mp 245 ºC (dec.). Found: C, 52.84; H, 3.97; N, 13.27. Calc. for $C_{56}H_{48}Ag_2B_2F_8N_{12}$: C, 52.61; H, 3.78; N, 13.15 %.

*[Ag$_2$(**2**)$_2$](PF$_6$)$_2$·CH$_2$Cl$_2$*

Silver hexafluorophosphate (23.9 mg, 0.095 mmol) in methanol (5 mL) was added to **2** (20.3 mg, 0.046 mmol) in dichloromethane/methanol (1:1; 8 mL). The colourless crystals which formed were collected, washed with dichloromethane and methanol. These crystals were suitable for X-ray crystallography. The remaining crystals were dried under vacuum before microanalysis. Yield 27.5 mg (68%); mp 239-240 ºC (dec.). Found: C, 41.76; H, 3.09; N,10.27. Calc. for $C_{28}H_{24}AgF_6N_6P{\cdot}CH_2Cl_2$: C, 41.55; H, 3.25; N, 9.69 %.

*[Ag(**3**)(NO$_3$)]*

Silver nitrate (15.8 mg, 0.093 mmol) in methanol (5 mL) was added to **3** (19.9 mg, 0.045 mmol) in dichloromethane/methanol (1:1; 8 mL). The colourless crystals which formed on slow evaporation of the above solution were collected, and washed with dichloromethane and methanol. A crystal from this crop was used for the X-ray crystallographic study. The remaining crystals were dried under vacuum before microanalysis. Yield, 22.6 mg (82%); mp 232-235 ºC (dec.). Found: C, 54.78; H, 3.84; N, 16.21. Calc. for $C_{28}H_{24}Ag\ N_7O_3$: C, 54.74; H, 3.94; N, 15.96 %.

*{[Ag(**3**)(CH$_3$CN)](ClO$_4$)}$_n$*

Silver perchlorate (16.8 mg, 0.099 mmol) in acetonitrile (5 mL) was added to **3** (28.1 mg, 0.063 mmol) in dichloromethane solution (5 mL). Colourless crystals of the title compound were obtained by slow diffusion of ether vapour into the resulting solution. A crystal from this crop was used for the X-ray structure determination. The remaining crystals were collected, washed with ether, and dried under vacuum. Yield, 14.5 mg (86%); mp 233-235 ºC. Found: C, 51.95; H, 3.78; N, 13.99. Calc. for $C_{28}H_{24}AgClN_6O_4 \cdot CH_3CN$: C, 51.99; H, 3.94; N, 14.15 %.

*{[Ag(**3**)(CH$_3$OH)](PF$_6$)·H$_2$O}$_n$*

Silver hexafluorophosphate (24.4 mg, 0.097 mmol) in methanol (5 mL) was added to a dichloromethane/methanol solution (1 : 1; 8 mL) of **3** (20.7 mg, 0.047 mmol). On standing, colourless crystals grew in the reaction mixture. These were collected and washed with dichloromethane and methanol. A crystal from this crop was used for the X-ray crystallography. The remaining crystals were dried in a vacuum before microanalysis. Yield, 11.0 mg (31%); mp 179-181 ºC (dec.). Found: C, 46.93; H, 3.87; N, 11.61. Calc. for $C_{28}H_{24}AgF_6N_6P \cdot CH_3OH \cdot H_2O$: C, 46.60; H, 4.05; N, 11.24 %.

*[Ag(**5**)(NO$_3$)]*

Silver nitrate (16.7 mg, 0.098 mmol) in methanol (5 mL) was added to **5** (20.5 mg, 0.046 mmol) in dichloromethane/methanol (1:1; 8 mL). A pale yellow crystalline solid formed following slow evaporation of the reaction mixture. This was collected, washed with

dichloromethane and methanol, and dried in a vacuum. Yield 27.5 mg (97 %). Found C, 54.85; H, 3.87; N, 16.02. Calc. for $C_{28}H_{24}N_7O_3Ag$: C, 54.74; H, 3.94; N, 15.96 %.

*[Ag_2(**5**)](BF_4)$_2$*

Silver tetrafluoroborate (19.3 mg, 0.099 mmol) in methanol (5mL) was added to **5** (19.8 mg, 0.045 mmol) in dichloromethane/methanol (1 : 1; 8 mL). Pale yellow crystals formed. These were collected, washed with dichloromethane and methanol, and then dried under vacuum. Yield 14.5 mg (39 %). Found: C, 41.03; H, 2.94; N, 10.13. Calc. for $C_{28}H_{24}N_6B_2F_8Ag_2$: C, 40.33; H, 2.90; N, 10.08 %.

*[Ag(**5**)](PF_6)·CH_3OH*

Silver hexafluorophosphate (25.8 mg, 0.102 mmol) in methanol (5 mL) was added to **5** (20.5 mg, 0.046 mmol) in dichloromethane/methanol (1 : 1; 8 mL). A yellow crystalline solid formed. This was collected, washed with dichloromethane and methanol, and dried in a vacuum. Yield 32.2 mg (95 %). Found: C, 48.08; H, 4.35; N, 11.55. Calc. for $C_{28}H_{24}N_6PF_6Ag{\cdot}CH_3OH$: C, 47.75; H, 3.87; N 11.52 %. Subsequently, further pale yellow crystals, suitable for X-ray crystallography, were isolated from the filtrate; the structure determination revealed that these have a different composition to that of the bulk sample, namely: $[Ag_3(\mathbf{5})_2(H_2O)](PF_6)_3{\cdot}2.5H_2O$.

*[Ag(**6**)(NO_3)]*

Silver nitrate (21.1 mg, 0.125 mmol) in acetonitrile (5 mL) was added to **6** (26.1 mg, 0.042 mmol) in dichloromethane (5 mL). Yellow crystals of the title compound were obtained by slow diffusion of diethylether vapour into the resulting solution. The crystals

were collected and washed with ether. Yield, 7.01 mg (33 %); mp 210-212 °C (dec.). Found: C, 58.53; H, 4.13; N, 17.66. Calc. for $C_{39}H_{33}N_{10}AgO_3$: C, 58.73; H, 4.17; N, 17.56 %. MS (ESI) m/z = 735.3 $[L+Ag]^+$.

Liquid–liquid extraction experiments

Liquid-liquid extraction experiments were performed at 23 ± 1 °C in microcentrifuge tubes (2 cm³) with a phase ratio $V_{(org)} : V_{(aq)}$ of 1 : 1 (500 μL each) with the silver in each phase measured radiometrically by γ-emission of ^{110m}Ag by means of a NaI (TI) scintillation counter (Cobra/Canberra-Packard). The aqueous phase contained Ag(I) perchlorate (1×10^{-4} M), a supporting anion (either sodium nitrate (5×10^{-3} M), sodium perchlorate (5×10^{-3} M) or picric acid (5×10^{-3} M)) and a selected buffer. The zwitterionic buffer system, MES/NaOH, was used to maintain a pH of 6.2 in the organic phase; as a precaution, the pH of the aqueous phase was measured before and after each experiment using a InLab423 pH electrode. The organic phase contained a known concentration of ligand in chloroform (normally 1×10^{-3} M except where variable concentration experiments were employed). All experiments involved the mechanical shaking of the two-phase system for 30 min by which time equilibrium was reached. At the end of this time, the phases were separated, centrifuged and then duplicate 100 μL samples of the aqueous and organic phases were removed for analysis.

Membrane transport

The transport experiments employing **1**-**6** as ionophores were carried out using a ‘concentric cell’ in which the aqueous source phase (10 mL) and receiving phase (30 mL)

were separated by a chloroform phase (50 mL). Details of the cell design have been published previously.[20] For each experiment both the aqueous phases and the organic phase were stirred separately at 10 rpm; the cell was enclosed by a water jacket and thermostatted at 25 °C. The aqueous source phase was buffered (CH_3CO_2H–CH_3CO_2Na) at pH 4.9 (±0.1) (6.95 mL of 2 M sodium acetate solution and 3.05 mL of 2 M acetic acid made up to 100 mL) and contained an equimolar solution of the nitrate salts of Co(II), Ni(II), Zn(II), Cu(II), Cd(II), Pb(II) and Ag(I), each at a concentration of 1×10^{-2} M. The chloroform phase contained the ligand at 1×10^{-3} M. The aqueous receiving phase was buffered (HCO_2H–HCO_2Na) at pH 3.0 ± 0.1 (56.6 mL of 1 M formic acid and 10.0 mL of 1 M sodium hydroxide made up to 100 mL). All transport runs were terminated after 24 h and atomic absorption spectroscopy was used to determine the amount of metal ion transported over this period. Transport rates (*J* values) are in mol ($24\ h^{-1}$). The transport results are quoted as the average values obtained from duplicate runs (error *ca.* ±10% of reported value).

X-ray structure determinations

Crystals employed for the X-ray determinations were obtained directly from the respective reaction solutions and were used without further drying. Structures of **2**, $\{[Ag(\mathbf{3})(CH_3CN)]\cdot(CH_3CN)\cdot(ClO_4)\}_n$ and $[Ag_2(\mathbf{3})_2(ClO_4)_2]\cdot 2H_2O$ were collected on a Nonius Kappa CCD with ω and ψ scans to approximately 56° 2θ at 198(2) K. Data collections were undertaken with COLLECT,[21] cell refinement with Dirax/lsq,[22] data reduction with EvalCCD[23] and structure solution with SHELXS-97.[24] Structures of **5,** $[Ag_2(\mathbf{2})_2(NO_3)_2]$, $[Ag_2(\mathbf{2})_2](BF_4)_2$, $\{[Ag_2(\mathbf{2})_2](PF_6)_2\}_3\cdot 2CH_2Cl_2\cdot 2CH_3OH$, $[Ag(\mathbf{3})(NO_3)]$,

{[Ag(**3**)(CH_3OH)](PF_6)}$_n$ and [Ag_3(**5**)$_2$(H_2O)](PF_6)$_3$·2.5H_2O, were collected at 168(2) K with a Bruker CCD area detector with ω and ψ scans to approximately 53° 2θ. Data integration and reduction were undertaken with SAINT and XPREP.[25] The structures were solved by direct methods using SHELXS-97.[24] Structures of **3** and [Ag(**6**)NO_3] were collected at 150(2) K with ω scans to approximately 56° 2θ using a Bruker SMART 1000 diffractometer. Data integration and reduction were undertaken with SAINT and XPREP[25] and subsequent computations were carried out using the WinGX-32 graphical user interface.[26] These structures were solved by direct methods using SIR97[27] All three diffractometers employed graphite-monochromated Mo-K*a* radiation generated from a sealed tube (0.71073 Å), Multi-scan empirical absorption corrections were applied to all data sets, where appropriate, using the program SADABS.[28] All structures were refined and extended with SHELXL-97.[29] In general, ordered non-hydrogen atoms with occupancies greater than or equal to 0.5 were refined anisotropically. Partial occupancy carbon, nitrogen and oxygen atoms were refined isotropically. Carbon-bound hydrogen atoms were included in idealised positions and refined using a riding model. Oxygen-bound hydrogen atoms that were structurally evident in the difference Fourier map were included and refined with bond length and angle restraints.

Crystal data

Crystal and structure refinement data for all structures are summarised in Table 1. ORTEP[30] depictions of the crystal structures are given in Figs.1-3 and are also provided in Figs. S2, S3 and S5 in the ESI† while schematic depictions of structures are shown in Figs. 4-12, S1 and S4. Where applicable, additional details relating to the X-ray crystal

structure refinement are given in the ESI† (along with tables of selected bond lengths and angles).

Results and Discussion

The 2,2′-dipyridylamine ligands **1–3** and **5-6** were prepared by the reaction of 2,2′ dipyridylamine with the appropriate alkyl halide derivative in the presence of base; while the synthesis of **4** has been reported elsewhere by our group.[18] In order to investigate the silver ion chemistry of **1-6** and make structural comparisons between these derivatives and their resulting silver complexes, an attempt was made to obtain crystalline products suitable for X-ray diffraction of both the ligands and their corresponding complexes. Solid complexes of type $[Ag(\mathbf{1})(NO_3)]\cdot CH_3CN$, $[Ag_2(\mathbf{2})_2(NO_3)_2]\cdot 2H_2O$, $[Ag_2(\mathbf{2})_2(ClO_4)_2]\cdot CH_3CN$, $[Ag_2(\mathbf{2})_2](BF_4)_2$, $[Ag_2(\mathbf{2})_2](PF_6)_2\cdot CH_2Cl_2$, $[Ag(\mathbf{3})(NO_3)]$, $\{[Ag(\mathbf{3})(CH_3CN)]ClO_4)_n$, $\{[Ag(\mathbf{3})(CH_3OH)]PF_6\cdot H_2O\}_n$, $[Ag(\mathbf{5})NO_3]$, $[Ag_3(\mathbf{5})_2(H_2O)](PF_6)_3\cdot 2.5H_2O$, $[Ag_2(\mathbf{5})](BF_4)_2$, $[Ag(\mathbf{5})]PF_6\cdot CH_3OH$ and $[Ag(\mathbf{6})NO_3]$ were isolated following the reaction of the appropriate silver salt in methanol or acetonitrile with the required ligand in dichloromethane and/or methanol. We have also recently reported the synthesis of the related complex, $[Ag_2(\mathbf{4})CH_3CN]_2[Ag_2(NO_3)_6]\cdot 0.75CH_3CN\cdot 0.25CH_2Cl_2$.[18]

X-ray structures of ligands 2, 3 and 5

Suitable crystals for X-ray structure analysis of the isomeric bis(di-2-pyridylaminomethyl)benzenes **2**, **3** and **5** were obtained. The structure of **2** is presented in Fig. 1. The aliphatic nitrogen atoms associated with each of the dpa moieties in this

structure are considerably distorted from the usually observed trigonal pyramidal arrangement for simple tertiary amines towards a more trigonal planar geometry – undoubtedly reflecting electron-pair delocalisation that also involves the attached aromatic rings, resulting in the nitrogens showing some sp^2 character. Thus, the angles between the bonds to the pyridyl rings from the aliphatic nitrogen atoms (N(7) and N(22)), are 124 ° and 122 ° respectively.

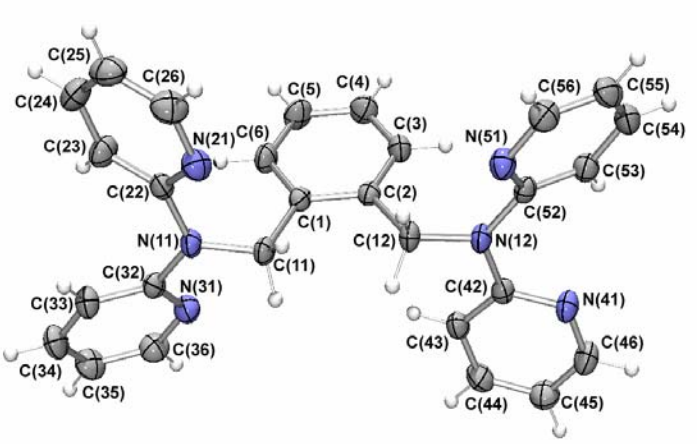

Fig. 1 ORTEP plot of **2** shown with 50 % probability ellipsoids.

The two pyridyl rings of each dpa moiety are not co-planar. In the N(7)-containing dpa moiety the two pyridyl rings are ‘reversed’ (that is approaching a 'trans' orientation) with respect to each other so that the ring nitrogens are not adjacent, while in the N(22)-containing fragment the two rings are oriented so that the nitrogen atoms are somewhat closer. Adjacent molecules pack in two dimensional sheets which propogate via a combination of phenylene to pyridyl nitrogen interactions and edge to face π-π interactions (Fig. S1).

The structure of **3** is shown in Fig. 2**.** Again the tertiary amines are considerably closer to a trigonal planar than a tetrahedral geometry with, for example, the angle

between the bonds from N(1) to the N(2)- and N(3)-containing rings in one dpa moiety being 121° while in the other (the N(4)-containing dpa fragment) the corresponding angle is 123°. Like the structure of **2** there are two arrangements of the dpa pyridyl rings present in this structure. The N(1)-containing moiety is arranged in a generally similar manner to that in the N(7)- containing moiety in the structure of **2**. The conformation of the N(4)-containing moiety is similar to the N(22)-containing fragment in the above structure, once again stabilised by the presence of weak nitrogen to hydrogen interactions in the structure. However, in contrast to **2** there is also evidence for π-π stacking in this structure. An intermolecular edge-to-face π-interaction occurs between the N(3)- and N(5)-containing rings, reflected by a H(25) to C(5) distance of 2.7 Å; a similar interaction, given by a H(28) to C(24) distance of 2.8 Å, also indicates the presence of an edge-to-face interaction between the N(5)- and N(6)-containing rings.

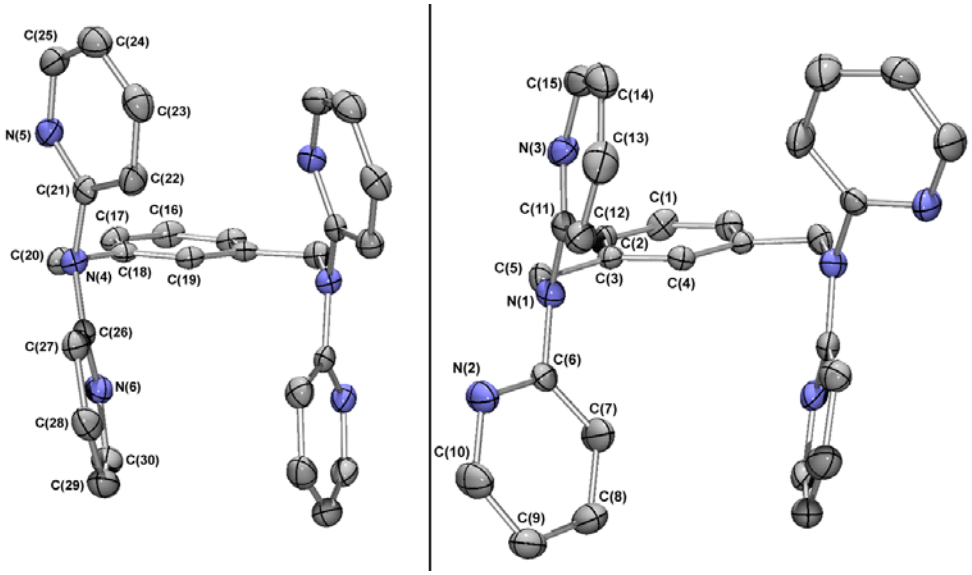

Fig. 2 ORTEP plots of **3** shown with 50 % probability ellipsoids. The asymmetric unit contains two crystallographically independent but chemically identical molecules, each

with crystallographic C_2 symmetry. Symmetry operators used for generating equivalent atoms: Left: -*x*+1, *y*, -*z*+1 Right: -*x*+1, *y*, -*z*

As shown in Fig. 3, the structure of **5** also contains tertiary amines that are almost planar, with the pyridyl moieties again oriented in a similar manner to those in the structures of **2** and **3**. Some edge-to-face π-π stacking is present between the N(21)- and N(31)-containing rings as well as between the N(21)-containing ring and the central arene ring. These are reflected by distances of 2.7 Å (H(36A)–C(26)) and 2.9 Å (H(26A)–C(6)) respectively. Again there are weak nitrogen-hydrogen interactions present which presumably aid in reducing the flexibility of the structure (see below).

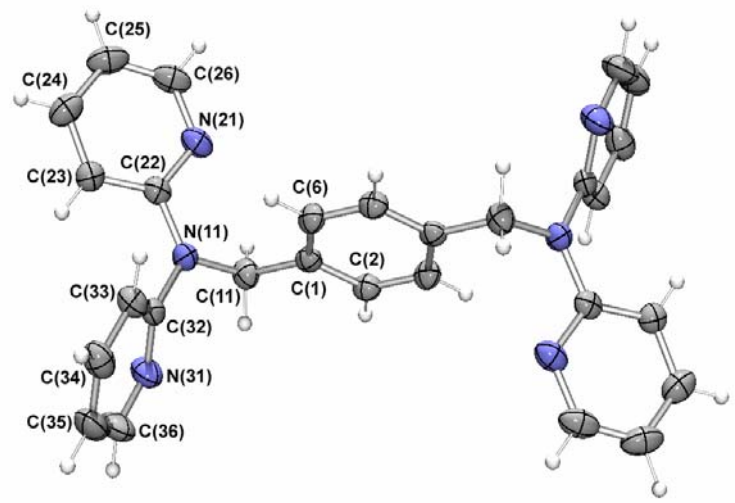

Fig. 3 ORTEP plot of **5** shown with 50 % probability ellipsoids. Symmetry operator used to generate equivalent atoms: -*x*+1, -*y*, -*z*+1

A common feature of each of the above ligand structures is that the tertiary nitrogens almost lie in the plane of the central substituted phenyl ring. This leads to close contacts between the aliphatic nitrogen atoms and adjacent aryl hydrogen atoms present on the phenylene cores. Namely, in **2** inter-atomic distances of 2.5 Å (H(16)–N(7)) and 2.5 Å (H(19)–N(22)) occur, in **3** distances of 2.5 Å (H(4)–N(1)) and 2.5 Å (H(19)–N(4)) are present while in **5** a distance of 2.6 Å (H(6A)–N(11)) occurs. Such distances are typical of interactions between phenyl hydrogens and amine nitrogens. Interactions of this type are well documented to play a role in structure stabilisation in other systems[31,32] and this also appears to be the case in the present solid state arrangements of **2**, **3** and **5**. Taken together with the tendency towards sp^2 hybridisation of the aliphatic nitrogens, such interactions will act to restrict the flexibility in these ligand systems. Any such decreased flexibility serves to add a degree of preorganisation to the respective structures which is also evident in the structures of the corresponding Ag(I) complexes in particular instances (see below).

X-Ray structures of Ag(I) complexes

Each Ag(I) ion in $[Ag_2(\mathbf{2})_2(NO_3)_2]$ (Fig. 4), has a four-coordinate, pseudo-tetrahedral geometry with a coordination sphere consisting of two pyridine N-donors from different ligands and a chelating nitrate anion. Thus only one of the pyridyl groups from each dpa unit is bound to a Ag(I) ion, while the second remains uncoordinated. This results in the formation of a discrete [2+2] metallacyclic structure. Other examples of dpa moieties failing to chelate to Ag(I) have also been documented.[4,5,33] Two weak silver-arene π-interactions involving the non-coordinated pyridine rings are present in the structure,

these presumably aid stabilisation of the complex and contribute to the overall rigidity of the system.

As observed for free **2,** the tertiary nitrogen groups of each dpa moiety are again distorted from ideal tetrahedral geometry towards trigonal planar and are similar to those observed in the crystal structure of free ligand **2**. There are also short contacts between phenylene hydrogen atoms and both tertiary amines, again stiffening the structure.

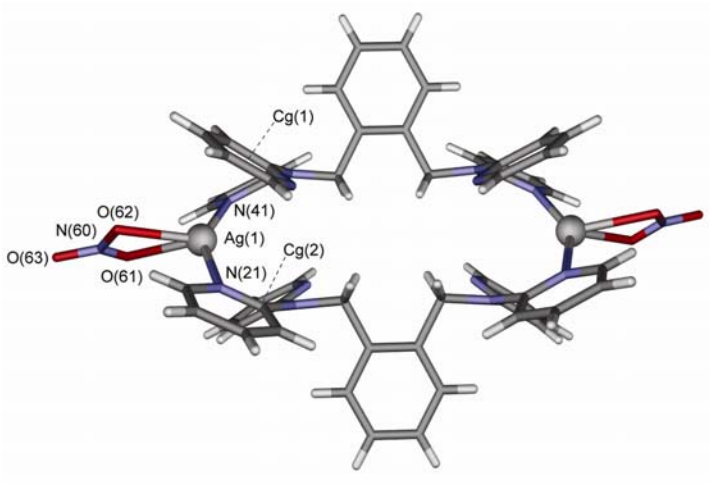

Fig. 4. A schematic representation of the X-ray crystal structure of $[Ag_2(\mathbf{2})_2(NO_3)_2]$ Ag(I) ions are shown as spheres. Ag(1)-Cg(1) 3.1 Å and Ag(1)-Cg(2) 3.3 Å. (Cg = ring centroid).

An investigation of the effect of variation of the anion on the resulting structure adopted in the solid state was carried out. Thus an analogous synthesis to that used to obtain $[Ag_2(\mathbf{2})_2(NO_3)_2]$ was repeated in which silver perchlorate was substituted for the nitrate salt. Reaction of two equivalents of $AgClO_4$ with **2** again resulted in a discrete [2+2] macrocyclic product of stoichiometry $[Ag_2(\mathbf{2})_2(ClO_4)_2]\cdot 2H_2O$ (Fig. 5). Despite the

addition of Ag(I) to **2** in a 2 : 1 ratio, only the above 2 : 2 complex was isolated. The X-ray structure of this product shows that each silver is bound to two pyridine N donors from different ligands and to one oxygen atom of the perchlorate in a trigonal planar geometry. The latter contrasts with the distorted tetrahedral geometry obtained with the nitrate anion. Nevertheless, the structure shows remarkable similarity to that of $[Ag_2(\mathbf{2})_2(NO_3)_2]$.

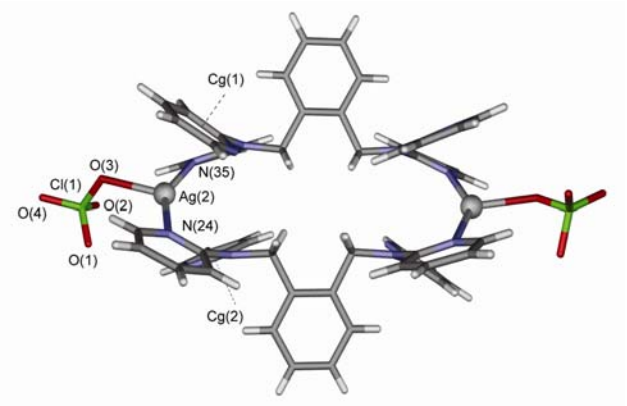

.

Fig. 5 A schematic representation of the X-ray crystal structure of $[Ag_2(\mathbf{2})_2(ClO_4)_2]\cdot 2H_2O$. Ag(I) ions are shown as spheres. Water molecules are not shown. Ag(1)-Cg(1) 3.2 Å, Ag(1)-Cg(2) 3.2 Å. (Cg = ring centroid).

In the presence of the non-coordinating anions, tetrafluoroborate or hexafluorophosphate, the complexes $[Ag_2(\mathbf{2})_2](BF_4)_2$ and $[Ag_2(\mathbf{2})_2]_3(PF_6)_6\cdot 2CH_2Cl_2\cdot 2CH_3OH$ were obtained. These were synthesised directly by the reaction of two equivalents of $AgBF_4$ or $AgPF_6$ with **2** and, as was observed for the nitrate and perchlorate salts, gave 2:2 complexes. As expected, the X-ray analysis of each species revealed that neither anion coordinates to a Ag(I) centre (Figs. **6** and **7**). In each

case the silver ions are each formally two-coordinate, again forming a [2+2] metallacycle with each silver bound to a pyridine donor from a different ligand. In the tetrafluoroborate case, the coordination to each silver involves a 'bent' two-coordinate geometry with, for example, the N(21A)–Ag(1)–N(41) bond angle being 152.84(7)º. Interestingly, there are some short range interactions present between both Ag(I) ions and a disordered tetrafluoroborate anion, with the presence of silver-fluorine distances of 2.681(2) and 2.686(2) Å.

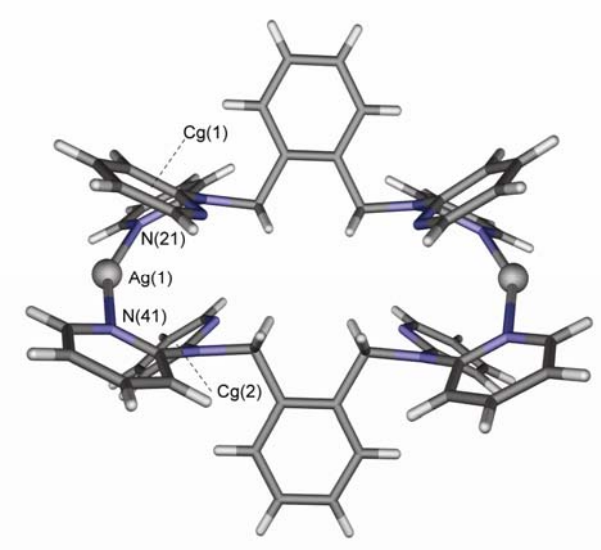

Fig. 6 A schematic representation of the X-ray crystal structure of $[Ag_2(\mathbf{2})_2](BF_4)_2$. Ag(I) ions are shown as spheres. Tetrafluoroborate anions are not shown. Ag(1)-Cg(1) 3.1 Å, Ag(1)-Cg(2) 3.2 Å (Cg = ring centroid).

Unlike the above structure, there are no silver-anion interactions present in $[Ag_2(\mathbf{2})_2]_3(PF_6)_6{\cdot}2CH_2Cl_2{\cdot}2CH_3OH$. However, pyridine coordination of the silver atom

(and hence the stability of the system) is complemented by intermolecular silver-π interactions between each silver and the uncoordinated pyridine rings of adjacent [2+2] metallocycles. These Ag–π interactions appear significant[11,34] and have Ag-ring centroid distances of 3.3 Å. Their presence results in the formation of an infinite sheet-like two-dimensional network (Fig.**7**). Once again the arrangement of the ligands in this complex shows similarities to that adopted by the free ligand.

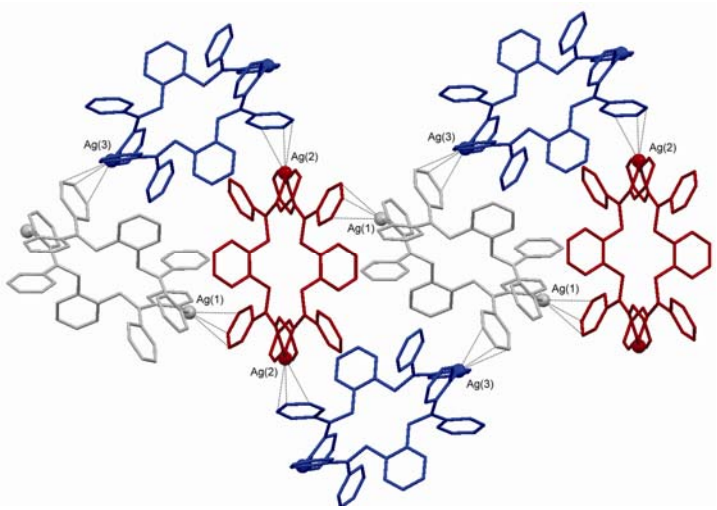

Fig. 7 A schematic representation of the Ag–π interactions in $[Ag_2(\mathbf{2})_2]_3(PF_6)_6{\cdot}2CH_2Cl_2{\cdot}2CH_3OH$, giving rise to a two-dimensional network.

Overall, the X-ray investigations show that all four of the complexes of **2** form 2 : 2 metallacyclic structures in which each dpa moiety bridges two silver ions irrespective of the anion present. Minor differences in the ring structure arise due to the coordination of NO_3^- or ClO_4^- anions to the silver centres while in the case of the BF_4^- and PF_6^- derivatives, (as expected) these anions do not coordinate, while essentially the same metallacyclic structural motif is maintained.

The reaction of **3** with AgX salts ($X = NO_3^-$, ClO_4^-, and PF_6^-) resulted in crystals suitable for X-ray analysis in each case. Variation of the reaction conditions (solvent type, anion present and/or ratio of metal ion to ligand employed) resulted in two very different structures forming; namely, a discrete [1+1] metallacycle and an infinite one-dimensional, polymeric chain species.

Discrete [Ag(**3**)(NO_3)] was obtained from the reaction of Ag(NO_3) with **3** in a 2 : 1 ratio in methanol/dichloromethane. As shown in Fig. 8, the resulting 1 : 1 complex has the Ag(I) in a distorted tetrahedral coordination environment composed of two pyridine N atoms from different dpa units and a chelating NO_3^- ion. As occurs for the other silver complex structures discussed so far, one 2-pyridyl ring from each dpa moiety does not participate in coordination; however, weak silver-π interactions with the non-coordinated pyridine rings and a silver-arene C–H interaction of 2.7 Å (involving H(2) of the central benzene core) help to stabilise the structure. Once again, short central phenylene hydrogen to tertiary nitrogen distances are present in this structure.

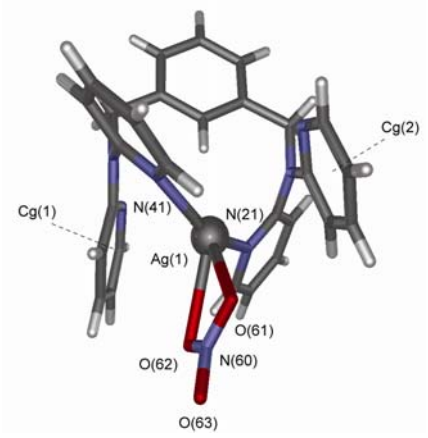

Fig. 8 A schematic representation of the X-ray crystal structure of [Ag(**3**)(NO_3)]. The silver ion is shown as a sphere. Ag(1)-Cg(1) 3.4 Å, Ag(1)-Cg(2) 3.4 Å (Cg = ring centroid).

The reaction of **3** with $AgPF_6$ and with $AgClO_4$ in a 1 : 2 ratio in methanol/dichloromethane and acetonitrile/dichloromethane, respectively, resulted in the isolation of corresponding one-dimensional coordination polymers of stoichiometries $\{[Ag(\mathbf{3})(CH_3OH)](PF_6)\}_n$ (Fig. 9) and $\{[Ag(\mathbf{3})(CH_3CN)](ClO_4)\cdot CH_3CN\}_n$ (Fig. 10). The Ag(I) in each case exhibits a distorted trigonal planar arrangement, with two sites coordinated to pyridyl moieties and the third to a methanol molecule (which is disordered over two sites) in the case of $\{[Ag(\mathbf{3})(CH_3OH)](PF_6)\}_n$, or an acetonitrile molecule in the case of $\{[Ag(\mathbf{3})(CH_3CN)](ClO_4)\cdot CH_3CN\}_n$. Again, in both products only one pyridyl group from each dpa unit coordinates to each silver ion and the structures are stabilised via weak offset face to face π-π and silver-π interactions.

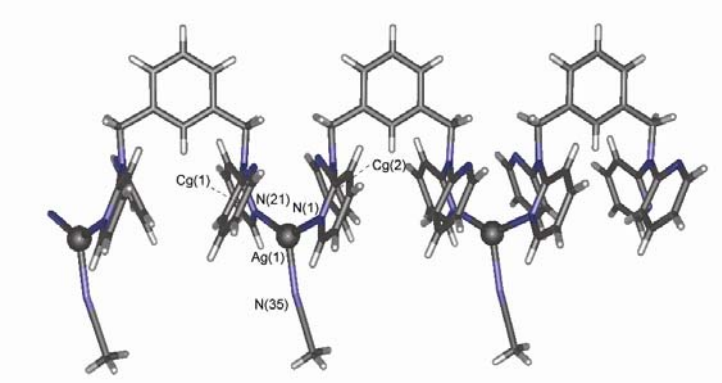

Fig. 9 The molecular structure of $\{[Ag(\mathbf{3})(CH_3OH)](PF_6)\}_n$. Hexafluorophosphate anions are not shown. Ag(1)-Cg(1) 3.3 Å (Cg = ring centroid).

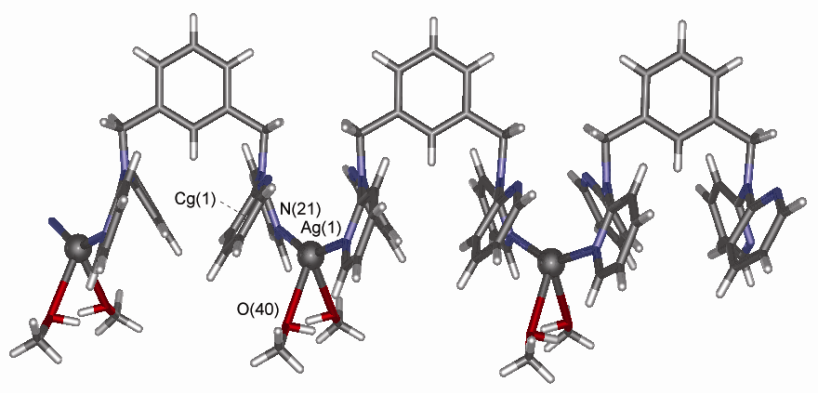

Fig. 10 The molecular structure of $\{[Ag(\mathbf{3})(CH_3CN)]ClO_4 \cdot CH_3CN\}_n$. The perchlorate anion and the non-coordinated acetonitrile are not shown. Ag(1)-Cg(1) 3.2 Å. Ag(1)-Cg(2) 3.4 Å (Cg = ring centroid).

The reaction of the 2,6-lutidinyl bridged, bis-dipyridylamine ligand **4** with silver nitrate in acetonitrile/dichloromethane results in polymeric species of type $\{[Ag_2(\mathbf{4})CH_3CN]_2(Ag_2(NO_3)_6) \cdot 0.75CH_3CN \cdot 0.25CH_2Cl_2\}_n$. The structure of this product incorporates a molecular ladder motif that consists of pairs of cationic $[Ag_2(\mathbf{4})CH_3CN]^{2+}$ units bridged by an unprecedented $[Ag_2(NO_3)_6]^{4-}$ anion.[18] The silver ions in the cationic dinuclear silver species are not equivalent. Each is bound to an oxygen from a 'terminal' nitrate group in an $[Ag_2(NO_3)_6]^{4-}$ unit. The coordination sphere of Ag(1) is completed by two pyridyl nitrogens from **4** and the lutidinyl nitrogen donor in a distorted tetrahedral arrangement. Ag(2) also has a distorted tetrahedral geometry with the coordination sphere composed of the remaining (two) pyridyl nitrogens from **4** and an acetonitrile molecule.

The structure of $[Ag_3(\mathbf{5})_2(H_2O)]PF_6)_3 \cdot 2.5H_2O$, generated from the reaction of $AgPF_6$ with **5** in a 2 : 1 ratio, is shown in Fig. 11**.** An M_3L_2 complex is formed, where at one end of the complex the di-2-pyridylamine units coordinate in a monodentate fashion towards one silver ion Ag(2), while at the opposite end, a twelve-membered

dimetallacycle is formed involving two silver ions (Ag(1)/Ag(3). The ligand strands have a helical twist between the Ag(2) and the Ag(1)/Ag(3) ends of the complex. The Ag(3) centre is also bound to a water molecule. The water molecule incorporating O(60) is hydrogen bonded to a nearby hexafluorophosphate anion and to a non-coordinated water molecule. Ag(3) is also involved in a silver–π interaction with an aryl ring of the ligand (Ag-C distances of 2.8 Å). Ag(1) and Ag(2) are only bound to pyridine nitrogens and show close to linear geometries; however, there are also weak contacts with the fluorine atoms of nearby hexafluorophosphate anions present. Silver-arene π-interactions involving Ag(1) and Ag(2) also occur.

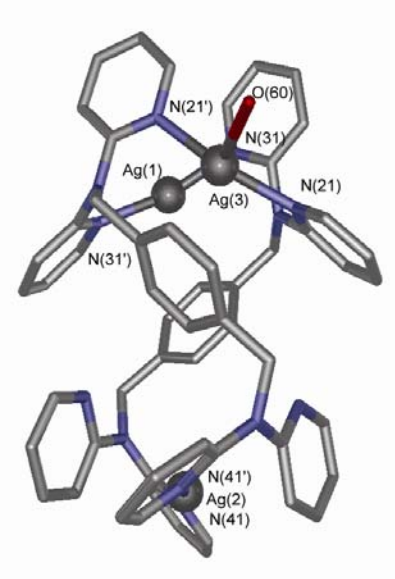

Fig. 11 The molecular structure of $[Ag_3(\mathbf{5})_2(H_2O)](PF_6)_3 \cdot 2.5H_2O$. Hexafluorophosphate anions and water molecules are not shown.

The reaction of **6** with Ag(I) nitrate in a 1:3 ratio results in the formation of a 1:1 (metal:ligand) complex $[Ag(\mathbf{6})(NO_3)]$. Like the structures discussed above, only one pyridyl from each pair of pyridyl rings is coordinated to silver (Fig. 12). A bidentate

nitrate anion is also bound such that the Ag(I) ion adopts a distorted tetrahedral geometry. No donors from the third dpa moiety are coordinated. As with the above structures, the central nitrogen of each dpa moiety exhibits a trigonal planar arrangement and lies close to the plane of the central aryl ring; the phenylene hydrogen to nitrogen interactions discussed previously are also present in this structure. The presence of the free dpa moiety suggests that this complex may be useful for the formation of extended heteronuclear structures on reaction with other metal ions.

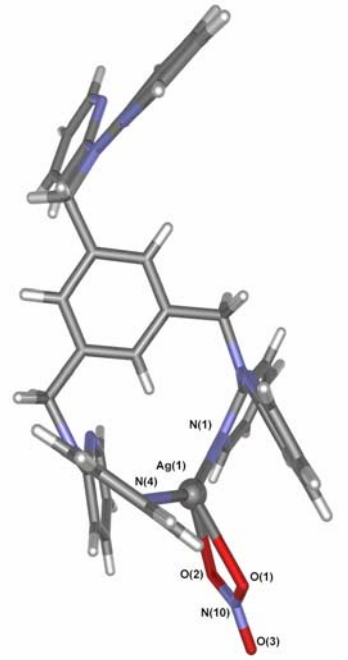

Fig. 12 The molecular structure of [Ag(**6**)(NO_3)].

Table 1 Crystal Data for the ligands **2**, **3**, and **5** and some of their complexes with Ag(I).

Compound	**2**	**3**	**5**	$[Ag_2(\mathbf{2})_2(NO_3)_2]$	$[Ag(\mathbf{3})(NO_3)]$	$\{[Ag(\mathbf{3})(CH_3CN)](ClO_4)\cdot CH_3CN\}_n$	$[Ag_3(\mathbf{5})_2(H_2O)](PF_6)_3\cdot 2.5H_2O$	$[Ag_2(\mathbf{2})_2](BF_4)_2$
Formula of Refinement Model	$C_{28}H_{24}N_6$	$C_{28}H_{24}N_6$	$C_{28}H_{24}N_6$	$C_{56}H_{48}Ag_2N_{14}O_6$	$C_{28}H_{24}AgN_7O_3$	$C_{32}H_{30}AgClN_8O_4$	$C_{56}H_{55}Ag_3F_{18}N_{12}O_{3.5}P_3$	$C_{56}H_{48}Ag_2B_2F_8N_{12}$
Molecular Weight	444.53	444.53	444.53	1228.82	614.41	733.96	1710.64	1278.42
Crystal System	Triclinic	Monoclinic	Monoclinic	Monoclinic	Triclinic	Monoclinic	Monoclinic	Monoclinic
Space Group	$P\bar{1}$	$C2$	$P2_1/n$	$P2_1/n$	$P\bar{1}$	$P2_1/c$	$P2_1/c$	$P2_1/n$
a / Å	9.218(1)	14.635(3)	8.483(2)	12.659(5)	8.8253(18)	8.522(1)	14.7918(9)	12.618(4)
b / Å	11.011(1)	9.2483(19)	16.999(4)	12.417(5)	10.437(2)	22.118(1)	14.7643(9)	12.798(4)
c / Å	12.294(1)	16.571(3)	8.759(2)	17.195(5)	14.732(3)	17.633(1)	29.0604(17)	17.110(6)
α / °	104.89(1)				85.759(2)			
β / °	95.32(1)	90.094(3)	115.643(3)	106.291(5)	84.787(2)	103.41(1)	94.881(1)	106.394(4)
γ / °	108.07(1)				70.861(2)			
V / Å^3	1126.08(18)	2243.0(8)	1138.6(5)	2594.3(16)	1275.2(4)	3233.0(4)	6323.5(7)	2650.8(15)
Dc / g cm^{-3}	1.311	1.316	1.297	1.573	1.600	1.508	1.797	1.602
Z	2	4	2	2	2	4	4	2
Crystal Size / mm	0.83 x 0.26 x 0.24	0.39 x 0.31 x 0.21	0.61 x 0.53 x 0.35	0.70 x 0.55 x 0.40	0.60 x 0.58 x 0.21	0.33 x 0.16 x 0.10	0.45 x 0.45 x 0.30	0.45 x 0.36 x 0.20
Crystal Colour	light yellow	colourless	pale yellow	colourless	colourless	colourless	brown	colourless
Crystal Habit	block	multi-face	Block	Block	block	block	block	block
Temperature / K	198(2)	150(2)	168(2)	168(2)	168(2)	198(2)	168(2)	168(2)
λ(MoKα)	0.71073	0.71073	0.71073	0.71073	0.71073	0.71073	0.71073	0.71073
μ(MoKα) /mm^{-1}	0.081	0.081	0.080	0.822	0.836	0.756	1.105	0.819
T(Empirical)$_{min,max}$	0.9360, 0.9809	N/A	0.7672 , 1.0000	0.8558, 1.0000	0.6367, 1.0000	0.9282, 0.7885	0.7908, 1.0000	0.7998, 1.0000
$2\theta_{max}$ / °	54.80	56.58	52.80	52.72	52.76	56.00	52.78	52.70
hkl range	-11 to 11, -14 to 14, -15 to 15	19 to18, -11 to12, -21 to 21	-10 to 10 , -21 to 21, -5 to 10	-15 to15, -15 to 15, 21 to 21	-10 to 10, -13 to 6, -18 to 18	-11 to 11, -29 to 29, -23 to 23	-12 to 18, -18 to 17, -27 to 36	-15 to 14, -15 to 15, -21 to 21
N	35395	10605	14413	31748	16279	73465	47897	32363
N_{ind} (R_{merge})	5013 (0.0376)	2821 (0.0268)	2292 (0.0160)	5275 (0.0191)	5067 (0.0211)	7770 (0.0380)	12819 (0.0328)	5348 (0.0374)
N_{obs} - ($I > 2\sigma$(I))	3900	2684	2102	4891	4815	6170	9727	4246
$R1^*$ - ($I > 2\sigma$(I)), $wR2^*$ - (all)	0.0395, 0.1037	0.0313, 0.0800	0.0403, 0.1024	0.0235, 0.0597	0.0234, 0.0626	0.0266, 0.0626	0.0395, 0.0980	0.0278, 0.0663
A^*, B^*	0.0534, 0.2205	0.0446, 0.4092	0.0481, 0.3332	0.0256, 1.8526	0.0398, 0.6586	0.0279, 1.7272	0.0471, 14.9391	0.0332, 1.5060
GoF	1.024	0.987	1.063	1.092	1.026	1.009	1.040	0.994
Residual Extrema / e$^-$ Å^{-3}	*0.218, -0.244*	0.147, -0.177	0.147, -0.161	0.574, -0.391	0.284, -0.688	0.363, -0.377	2.276, -1.385	0.466, -0.377

* $R1 = \Sigma||F_o| - |F_c||/\Sigma|F_o|$ for $F_o > 2\sigma(F_o)$ and $wR2 = \{\Sigma[w(F_o^2 - F_c^2)^2]/\Sigma[w(F_c^2)^2]\}^{1/2}$ where $w = 1/[\sigma^2(F_o^2) + (AP)^2 + BP]$, $P = (F_o^2 + 2F_c^2)/3$ and A and B are listed in the crystal data information supplied.

Table 1 (Cont.) Crystal Data for the remaining Ag(I) complexes.

Compound	$\{[Ag_2(\mathbf{2})_2](PF_6)_2\}_3 \cdot 2CH_2Cl_2 \cdot 2CH_3OH$	$[Ag_2(\mathbf{2})_2(ClO_4)_2] \cdot 2H_2O$	$\{[Ag(\mathbf{3})(CH_3OH)](PF_6)\}_n$	$[Ag(\mathbf{6})NO_3]$
Formula of Refinement Model	$C_{172}H_{156}Ag_6Cl_4F_{36}N_{36}O_2P_6$	$C_{56}H_{52}Ag_2Cl_2N_{12}O_{10}$	$C_{29}H_{28}AgF_6N_6OP$	$C_{39}H_{33}AgN_{10}O_3$
Molecular Weight	4418.16	1339.74	729.41	797.62
Crystal System	Triclinic	Orthorhombic	Monoclinic	Triclinic
Space Group	$P\bar{1}$	*Pccn*	*C*2/*c*	$P\bar{1}$
a / Å	14.361(5)	20.973(1)	8.623(3)	9.1320(15)
b / Å	17.001(6)	29.544(1)	25.164(9)	12.801(2)
c / Å	20.092(7)	17.798(1)	14.262(5)	15.264(3)
α / °	69.969(4)			81.910(3)
β / °	73.690(4)		94.626(4)	81.998(3)
γ / °	86.817(5)			71.440(3)
V / Å^3	4419(2)	11028.1(9)	3084.7(18)	1666.2(5)
*D*c / g cm^{-3}	1.660	1.614	1.571	1.590
Z	1	8	4	2
Crystal Size / mm	0.46 x 0.44 x 0.08	0.30 x 0.20 x 0.05	0.70 x 0.29 x 0.28	0.138 x 0.123 x 0.096
Crystal Colour	colourless	Colourless	colourless	yellow
Crystal Habit	plate	Plate	rod	block
Temperature / K	168(2)	198(2)	168(2)	150(2)
λ(MoKα)	0.71073	0.71073	0.71073	0.71073
μ(MoKα) /mm^{-1}	0.870	0.879	0.775	0.663
T(Empirical)$_{min,max}$	0.7133, 1.0000	0.7785, 0.9574	0.8307, 1.0000	0.745, 0.938
$2\theta_{max}$ / °	50.00	50.80	52.76	56.80
hkl range	-12 to 17 , -18 to 20 , -23 to 22	-23 to 25, -35 to 35, -16 to 21	-10 to 10, -30 to 31, -10 to 17	-12 to 12, -16 to 17, -20 to 20
N	51734	44563	17476	16508
N_{ind} (R_{merge})	15404 (0.0952)	9832 (0.0380)	3121 (0.0289)	7771(0.0352)
N_{obs} - ($I > 2\sigma$(I))	9767	6090	2833	5892
$R1^*$ - ($I > 2\sigma$(I)), $wR2^*$ - (all)	0.0496, 0.1377	0.0628, 0.1747	0.0572, 0.1457	0.0424, 0.0921
A^*, B^*	0.0640, 0.0000	0.0597, 87.2719	0.0449, 17.7216	0.0433, 0.0000
GoF	0.941	1.053	1.228	1.032
Residual Extrema / e$^-$ Å^{-3}	1.045, -1.063	1.375, -1.500	0.720, -1.188	-0.365, 0.628

* $R1 = \Sigma||F_o| - |F_c||/\Sigma|F_o|$ for $F_o > 2\sigma(F_o)$ and $wR2 = \{\Sigma[w(F_o^2 - F_c^2)^2]/\Sigma[w(F_c^2)^2]\}^{1/2}$ where $w = 1/[\sigma^2(F_o^2) + (AP)^2 + BP]$, $P = (F_o^2 + 2F_c^2)/3$ and *A* and *B* are listed in the crystal data information supplied.

Liquid–liquid extraction studies

The extraction behaviour of the di-2-pyridylaminomethylbenzene derivatives **1**–**6** towards Ag(I) was studied using the radiotracer technique.[35] A summary of the extraction results for each of **1**–**6** under comparable experimental conditions in the presence of different counterions in the aqueous phase is given in Fig. 13.

As expected there are pronounced differences in the extraction properties between **1** – **6**. We consider first the results obtained in the presence of perchlorate. In the case of the monosubstituted dpa derivative **1**, no Ag(I) extraction was detected while the (*ortho*- and *meta*-linked) bis-dpa derivatives **2** and **3** gave extraction values of 22 % and 14 % respectively and the corresponding 2,6-lutidinyl bridged, bis-dpa system **4** yielded a value of 44 %. Increasing the number of dpa residues to three in **6** leads to a further enhancement of extraction efficiency, with the value now being 54%. Interestingly, the para-disubstituted isomer of **2** and **3**, namely **5**, shows only trace extraction of Ag(I) into the organic phase. Ligand **4,** incorporating an additional pyridine donor function, extracted silver (44%) more efficiently when compared to its analogue ligand **3** (14%).

More lipophilic systems may aid the extraction process by inhibiting the bleeding of the amine ligand or its metal complex from the organic to the aqueous phase as well as enhancing extraction through favorable solvation effects. As is clearly evident from Fig. 14, the use of picrate improves the extraction efficiency over perchlorate which in turn yields significantly better extraction than nitrate. This is undoubtedly a reflection of the different lipophilicities of these anions and thus follows the expected anion influence on metal extraction predicted by the well-known Hofmeister series.[36]

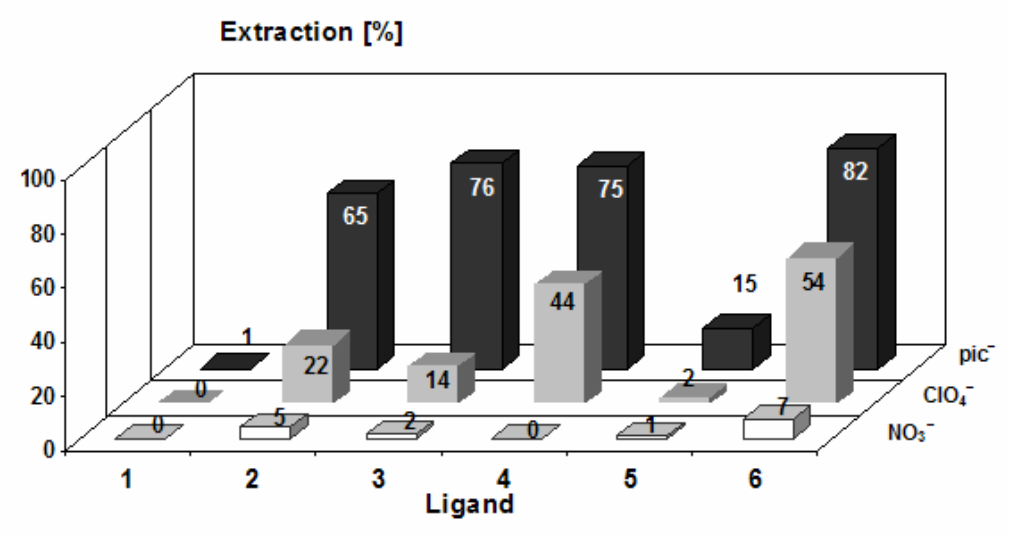

Fig. 13 Percent Ag(I) extraction by **1**–**6** with nitrate, perchlorate and picrate as the anion. $[AgNO_3] = 1 \times 10^{-4}$ M, $[NaNO_3] = 5 \times 10^{-3}$ M; $[AgClO_4] = 1 \times 10^{-4}$ M, $[NaClO_4] = 5 \times 10^{-3}$ M; $[AgNO_3] = 1 \times 10^{-4}$ M, [Hpic] = 5×10^{-3} M; pH 6.2 (MES/NaOH buffer); [ligand] = 1×10^{-3} M in $CHCl_3$; shaking time 30 min; T = 23 ± 1°C.

In order to investigate the stoichiometries of the extracted species, extraction experiments were performed in which the concentration of the ligand was varied while the metal ion concentration was maintained at 1×10^{-4} M and the anion concentration was effectively constant. The log $D_M = [M^{n+}]_{(org)}/[M^{n+}]_{(aq)}$ was then plotted against the log of the ligand concentration. Provided a 'simple' equilibrium is involved, the slope of this plot gives the stoichiometry of the extracted species directly.[37]

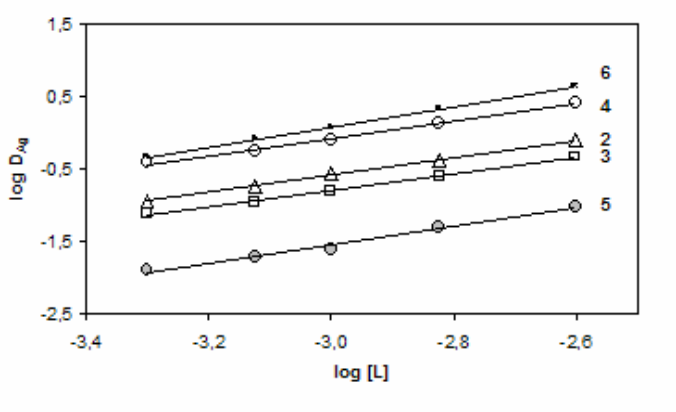

Fig. 14 Variable ligand concentration experiments for **2**–**6** with Ag(I) and perchlorate as the anion. $[AgClO_4] = 1 \times 10^{-4}$ M, $[NaClO_4] = 5 \times 10^{-3}$ M; pH 6.2 (MES/NaOH buffer); [ligand]= 5×10^{-4} M – 2.5×10^{-3} M in $CHCl_3$; shaking time 30 min; T = 23 ± 1°C. Slopes: **6,** s = 1.40; **4,** s = 1.19; **2,** s = 1.19; **3,** s = 1.16; **5,** s = 1.29.

The results show linear relationships between the logarithms of the distribution ratio (D_{Ag}) and the ligand concentration (pH 6.2, ligand excess) (Fig. 14). Slopes of *ca.* 1.2 were obtained for **2**, **3**, and **4** and hence indicate approximate 1 : 1 Ag(I) : L stoichiometries in each of these cases. This stoichiometry corresponds with that observed in the X-ray crystal structures of the Ag(I) complexes of **2** and **3** in the solid state which have formulas of $[Ag_2(\mathbf{2})_2(ClO_4)_2]\cdot 2H_2O$ and $\{[Ag(\mathbf{3})(CH_3CN)](ClO_4)\cdot CH_3CN\}_n$ respectively (but not for **4** where the solid state stoichiometry is given by $\{[Ag_2(\mathbf{4})CH_3CN]_2(Ag_2(NO_3)_6)\}$). In contrast, the slopes obtained for ligands **5** and **6** fall a little higher at 1.29 and 1.40 respectively and hence suggest that more complex solution stoichiometries/equilibria occur in these cases.

Bulk membrane transport studies

Competitive mixed metal transport experiments across a bulk chloroform membrane (water/chloroform/water) have been undertaken. The chloroform membrane phase contained the ionophore at 1×10^{-3} M chosen from **1**–**6**, respectively. The aqueous source phase contained equimolar concentrations of the nitrate salts of Co(II), Ni(II), Cu(II), Zn(II), Cd(II), Ag(I) and Pb(II), with individual metal ion concentrations being 1×10^{-2} M. As mentioned in the Experimental, transport was performed against a back gradient of protons. Under the conditions employed (and ignoring any apparent transport showing J values $<15 \times 10^{-7}$ mol/24 h as being within experimental error of zero), sole selectivity for Ag(I) was observed for each of the ionophores **2**, **3**, **4** and **6**, with no transport of any ion occurring for **1** and **5** (Fig. 15).

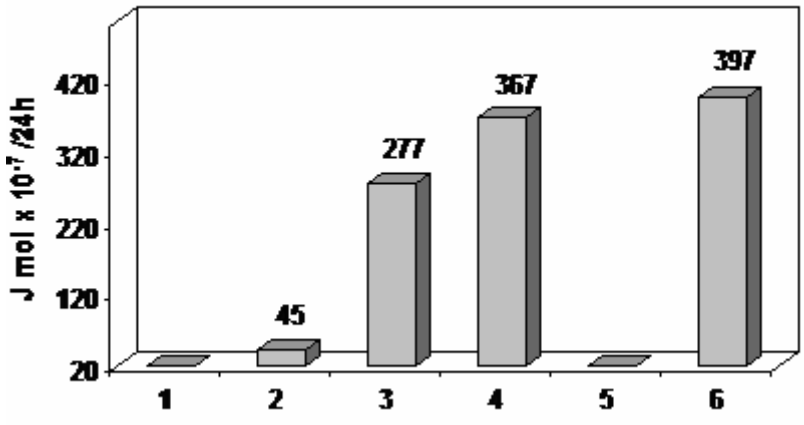

Fig. 15 Transport fluxes for Ag(I) in seven-metal competitive transport across a bulk $CHCl_3$ membrane employing **1**–**6** as ionophores (25°C).

Equimolar concentrations of Co(II), Ni(II), Cu(II), Zn(II), Cd(II), Ag(I), Pb(II) were initially present in the aqueous source phase; each metal had a concentration of 1×10^{-2} M, prepared in a buffer solution (CH_3CO_2H–CH_3CO_2Na) at pH 4.9 (±0.1). Under the

conditions employed (see Experimental), where transport occurred, sole transfer of Ag(I) into the aqueous receiving phase was observed.

Transport flux values for Ag(I) are illustrated in Fig.16. In parallel to the solvent extraction results for this ion, the monosubstituted dpa ligand **1** fails to act as ionophore for all seven metals under the conditions employed. The isomeric ligands incorporating two 2,2′-dipyridylamine units **2** ($J = 45 \times 10^{-7}$ mol/24 h) (*ortho* substituted) and **3** ($J = 277 \times 10^{-7}$ mol/24 h) (*meta* substituted) both promote significant Ag(I) transport (in parallel with their solvent extraction behaviour - although theory dictates that this need not necessarily be the case) but nevertheless they give quite different values indicating the influence of the different substitution positions on the 'linking' aryl ring. Indeed, for the corresponding *para* derivative **5,** no metal-ion transport was observed under the conditions employed – again this parallels the extraction results where this ligand was shown to be an inferior extractant of Ag(I) relative to the *ortho* and *meta*-linked isomers **2** and **3** (see Fig.13). Ligands **4** and **6** also yield results that broadly mimic those obtained in the corresponding solvent extraction experiments. Ionophore **4**, incorporating an additional pyridine donor function relative to **3**, acts as an efficient transporter of Ag(I) ($J = 367 \times 10^{-7}$ mol/24 h) whereas the tri-substituted derivative **6** was found to show the highest transport efficiency towards this ion – a J value of 397×10^{-7} mol/24 h was obtained.

Concluding Remarks

The Ag(I) chemistry of a series of linked dipyridylamine derivatives in both the solid state and solution has been explored. These ligands have been demonstrated to yield a

range of new silver complex derivatives showing both discrete and polymeric architectures. In solution, structure/function relationships underlying the interaction of these species with Ag(I) have been probed. In seven-metal competitive transport experiments across bulk chloroform membranes several of the ligands were demonstrated to show sole selectivity for Ag(I) over the remaining six transition and post transition metal ions present in the aqueous source phase.

Acknowledgements

We thank the Australian Research Council, the Royal Society of New Zealand Marsden Fund and the Deutsche Forschungsgemeinschaft for support. B.A. gratefully acknowledges the Max-Buchner-Stiftung for a research grant. O. K. acknowledges the DFG for assistance under grant 436RUS 17/20/06.

References

1. (*a*) P. Gamez, P. de Hoog, O. Roubeau, M. Lutz, W. L. Driessen, A. L. Spek and J. Reedijk, *Chem. Commun.*, 2002, 1488; (*b*) P.Gamez, P. de Hoog, M. Lutz, A. L. Spek and J. Reedijk, *Inorg. Chim. Acta*, 2003, **351**, 319; (*c*) P. de Hoog, P. Gamez, M. Leuken, O. Roubeau, B. Krebs and J. Reedijk, *Inorg. Chim. Acta,* 2004, **357**, 213; (*d*) S. Demeshko, G. Leibeling, S. Dechert and F. Meyer, *Dalton Trans.,* 2004, 3782; (*e*) C. Seward, W.-l. Jia, R.-Y. Wang and S. Wang, *Inorg.*

Chem., 2004, **43**, 978; (*f*) J.-S. Yang, Y.-D. Lin, Y.-H. Lin and F.-L. Liao, *J. Org. Chem.,* 2004, **69**, 3517.

2. W.-L. Jia, D.-R. Bai, T. McCormick, Q.-D. Liu, M. Motala, R.-Y. Wang, C. Seward, Y. Tao and S. Wang, *Chem. Eur. J.,* 2004, **10**, 994.

3. (*a*) J. Pang, Y. Tao, S. Freiberg, X.-P. Yang, M. D'Iorio and S. Wang, *J. Mater. Chem.*, 2002, **12**, 206; (*b*) C. Seward, J. Pang and S. Wang, *Eur. J. Inorg. Chem.,* 2002, 1390; (*c*) Q.-D. Liu, W.-L. Jia, G. Wu and S. Wang, *Organometallics*, 2003**, 22***,* 3781; (*d*)L. Aubouy, P. Gerbier, N. Huby, G. Wantz, L. Vignau, L. Hirsch and J.-M. Janot, *New J. Chem.*, 2004, **28**, 1086; (*e*) J.-S. Yang, Y.-D. Lin, Y.-H. Chang and S.-S. Wang, *J. Org. Chem.,* 2004, **70**, 6066

4. Y. Kang, C. Seward, D. Song and S. Wang, *Inorg. Chem.*, 2003, **42**, 2789.

5. C. Seward, W.-L. Jia, R.-Y. Wang, G. D. Enright and S. Wang, *Angew. Chem. Int. Ed*., 2004, **43**, 2933.

6. (*a*) A. K. Paul, H. Mansuri-Torshizi, T. S. Srivastava, S. J. Chavan and M. P. Chitnis, *J. Inorg. Biochem.*, 1993, **50**, 9; (*b*) I. Puscasu, C. Mock, M. Rauterkus, A. Rondigs, G. Tallen, S. Gangopadhyay, J.E.A. Wolff and B. Krebs, *Z. Anorg. Allg. Chem.*, 2001, **627**, 1292; (*c*) M. J. Rauterkus, S. Fakih, C. Mock, I. Puscasu and B. Krebs, *Inorg. Chim. Acta,* 2003, **350**, 355.

7. C. Tu, J. Lin, Y. Shao and Z. Guo, *Inorg. Chem.*, 2003, **42**, 5795.

8. S. Fakih, W. C. Tung, D. Eierhoff, C. Mock and B. Krebs, *Z. Anorg. Allg. Chem.*, 2005, **631**, 1397.

9. (*a*) P. J. Steel and C. J. Sumby, *Chem. Commun*., 2002, 322; (*b*) S. Hiraoka, T. Yi, M. Shiro and M. Shionoya, *J. Am. Chem. Soc*., 2002, **124**, 14510; (*c*) H.-J. Kim,

W.-C. Zin and M. Lee, *J. Am. Chem. Soc*., 2004, **126**, 7009; (*d*) O. B. Dolomanov, D. B. Cordes, N. R Champness, A. J. Blake, L. R. Hanton, G. B. Jameson, M. Schröder and C. Wilson, *Chem. Commun*., 2004, 642; (*e*) J. J. M. Amoore, C. A. Black, L. R. Hanton and M. D. Spicer, *Cryst. Growth & Design*, 2005, **5**, 1255; (*f*) P. Blondeau, A. van der Lee and M., Barboiu, *Inorg. Chem.*, 2005, **44**, 5649; (*g*) C. Shimokawa and S. Itoh, *Inorg. Chem*., 2005, **44**, 3010; (*h*) C. S. Purohit and S. Vema, *J. Am. Chem. Soc*., 2006, **128**, 400; (*i*) M. Munakata, L. P. Wu and T. Kuroda-Sowa, *Adv. Inorg. Chem.,* 1999, **46**, 173; (*j*) A. N. Khlobystov, A. J. Blake, N. R. Champness, D. A. Lemenovskii, A. G. Majouga, N. V. Zyk and M. Schröder, *Coord. Chem. Rev.,* 2001, **222**, 155; (*k*) S.-L. Zheng, M.-L. Tong and X.-M. Chen, *Coord. Chem. Rev*., 2003, **246**, 185; (*l*) C.-L. Chen, B.-S. Kang and C.-Y. Su, *Aust. J. Chem*., 2006, **59**, 3.

10 (*a*) M. Munakata, L. P. Wu and G. L. Ning, *Coord. Chem. Rev*., 2000, **198**, 171; (*b*) M. O. Awaleh, A. Badia and F. Brisse, *Cryst. Growth & Design,* 2005, **5**, 1897; (*c*) E. C. Constable, *Aust. J. Chem.*, 2006, **59**, 1; (*d*) L. R. Hanton and A. G. Young, *Cryst. Growth & Design*, 2006, **4**, 833.

11. Q.-M Wang and T. C. W. Mak, *Chem. Commun*., 2002, 2682.

12. (*a*) T.-T. Yeh, J.-Y. Wu, Y.-S. Wen, Y.-H. Liu, J. Twu, Y.-T. Tao and K.-L. Lu, *Dalton Trans*. 2005, 656; (*b*)Y.-B. Dong, Y. Geng, J.-P. Ma and R.-Q. Huang, *Inorg. Chem*., 2005**, 44**, 1693; (*c*) H. Hou, Y. Wei, Y. Song, L. Mi, M. Tang, L. Li and Y. Fan, *Angew. Chem. Int. Ed.*, 2005, **44**, 6067.

13. J.-H Liao, P.-L. Chen and C.-C. Hsu, *J. Phys. Chem. Solids,* 2001, **62**, 1629.

14. M. Burgos, O. Crespo, M. C. Gimeo, P. G. Jones and A. Laguna, *Eur. J. Inorg Chem.*, 2003, 2170.

15 C. Seward and S. Wang, *Comm. Inorg. Chem.*, 2005, **26**, 103.

16. T. Chao, Y. Shao, N. Gan, Q. Xu and Z. Guo, *Inorg. Chem.*, 2004, **43**, 4761.

17. (*a*) L. Song and W.C. Trogler, *J. Organomet. Chem.*, 1993, **452**, 271; (*b*) Y. Oh, *J. Korean Chem. Soc.*, 2000, **44**, 507.

18. B. Antonioli, D. J. Bray, J. K. Clegg, K. Gloe, K. Gloe, H. Heβke and L. F. Lindoy; *Chem Commum.*, 2006, submitted.

19. E. Diez-Barra, J.C. Garcia-Martinez, S. Merino, R. del Rey, J. Rodriguez-Lopez, P. Sanchez-Verdu and J. Tejeda, *J. Org. Chem*., 2001, **66**, 5664.

20. P. S. K. Chia, L. F. Lindoy, G. W. Walker and G. W. Everett, *Pure Appl. Chem.*, 1993, **65**, 521.

21. Nonium BV, Delft, The Netherlands, 1998.

22. A. J. M. Duisenberg, *J. Appl. Cryst.*, 1992, **25**, 92.

23. A. J. M. Duisenberg, L. M. J. Kroon-Batenburg and A. M. M. Schreurs, *J. Appl. Cryst*., 2003, **36**, 220.

24. G. M. Sheldrick, *Acta Cryst.*, 1990, ***A46***, 467.

25. Bruker (1995), SMART, SAINT and XPREP. Bruker Analytical X-ray Instruments Inc., Madison, Wisconsin, USA.

26. WinGX-32: System of programs for solving, refining and analysing single crystal X-ray diffraction data for small molecules, L. J. Farrugia, *J. Appl. Cryst.*, 1999, **32**, 837.

27. A. Altomare, M. C. Burla, M. Camalli, G. L. Cascarano, C. Giocavazzo, A. Guagliardi, A. G. C. Moliterni, G. Polidori and S. Spagna, *J. Appl. Cryst.,* 1999, **32**, 115.

28. G. M. Sheldrick, *SADABS: Empirical Absorption and Correction Software,* University of Göttingen, Germany, 1999-2003.

29. G. M. Sheldrick, *SHELXL-97: Programs for Crystal Structure Analysis*, University of Göttingen, Germany, 1997.

30. L. J. Farrugia, *J. Appl. Crystallogr.*, 1999, **30**, 565.

31. L. F. Lindoy and I. M. Atkinson, *Self-assembly in Supramolecular Chemistry.* RSC, Cambridge UK, 2000.

32. (*a*) G.A. Jeffery, *Cryst. Rev.,* 2003, **9**, 135; (*b*) S. F. Alshahateel, R. Bishop, D. C. Craig and M. L. Scudder, *Cryst. Eng. Comm.*, 2001, **55**, 1; (*c*) A. N. M. M. Rahman, R. Bishop, D. C. Craig and M. L. Scudder, *Eur. J. Org. Chem*., 2003, 72.

33. C. Seward, J. Chan, D. Song and S. Wang, *Inorg. Chem*., 2003, **42**, 1112.

34. X.-D. Chen and T.C.W. Mak, *J. Molec. Struct.*, 2005, **743**, 1.

35. K. Gloe and P. Mühl*, Isotopenpraxis*, 1983, **19**, 257.

36. F. Hofmeister, *Arch. Exp. Pathol. Pharmakol.*, 1888, **24**, 247.

37. J. Rydberg, G. R. Choppin, C. Musikas and T. Sekine, *Solvent Extraction Equilibria*, in Solvent Extraction Principles and Practice, J. Rydberg, M. Cox, C. Musikas and G. R. Choppin, Eds., Marcel Dekker, New York, **2004,** pp. 109.

Graphical Abstract

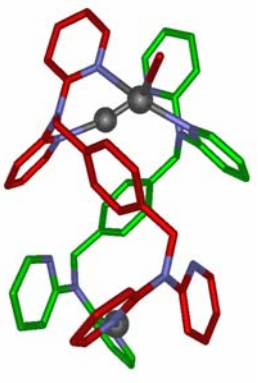

The interaction of Ag(I) with a series of linked dipyridylamine derivatives in both the solid state and solution has been investigated; these ligands yield a range of new silver complex derivatives showing both discrete and polymeric architectures.